

## Mode generation via interaction

Alexander M. Balk

*Department of Mathematics, University of Utah, 155 South 1400 East, Salt Lake City, Utah 84112, USA*



(Received 10 July 2018; published 11 December 2018)

This paper reports a robust regime in the dynamics of three coupled modes when one mode is pumped, the second is dissipated, and the third is not subject to any external action. In this regime, the first and the second modes vanish, while the third mode becomes large. This is applied to the problem of plasma confinement by magnetic field, when the third mode represents zonal (poloidal) flow. This paper demonstrates that in order to generate strong zonal (poloidal) flow—a transport barrier—in magnetically confined fusion plasma, it is beneficial to have significant decrement in addition to increment of other modes.

DOI: [10.1103/PhysRevE.98.062208](https://doi.org/10.1103/PhysRevE.98.062208)

### I. INTRODUCTION

In several problems, there is a necessity to generate a certain mode, which is not amenable to direct excitation by external sources. An example is generation of zonal (poloidal) flow in fusion devices with magnetic confinement. Such a flow is similar to zonal jets in atmospheres and oceans. The fluid turbulence is often strongly nonlinear and so roughly isotropic (anisotropy usually enters through linear terms in dynamical equations). The turbulent transport of a dye particle,  $\dot{\mathbf{r}} = \mathbf{v}(\mathbf{r}, t)$ , is characterized by the correlation length  $\xi$  of fluid turbulence: Roughly, the particle moves in a straight line with the typical fluid velocity  $v_*$  for time  $\tau = \xi/v_*$  and then randomly changes its direction. So, the turbulent diffusion has coefficient  $\xi^2/2\tau = v_*^2\tau/2$ . The presence of large-scale zonal jets [or zonal (poloidal) flow in plasma context] significantly decreases the north-south (or radial in plasma) turbulent transport (e.g., [1–7]). Such zonal flow could be generated by the turbulence itself or be added as a result of external generation. Anyway, if  $\psi(x, y, t)$  is the stream function of the generated fluid motion, the transport equations become

$$\dot{x} = -\frac{\partial\psi}{\partial y} + u(x, y, t), \quad \dot{y} = \frac{\partial\psi}{\partial x} + v(x, y, t), \quad (1)$$

$(x, y)$  are coordinates in the poloidal-zonal and the radial-meridional directions, and  $(u, v)$  are the respective velocities of fluid turbulence. The  $\psi$  field can have wavelike character and be clearly anisotropic. Even when the  $\psi$  field has significant magnitude, by itself it can provide little contribution to radial transport. [This depends on the topology of the streamlines of the  $\psi$  field (e.g., [8]); in particular, if the  $\psi$  field mainly represents poloidal (zonal) velocity, then it makes little contribution to radial velocity of passive tracer particles. Besides, if the  $\psi$ -field is a random wave field, then its turbulent diffusion is of the 4-th order in wave amplitudes, e.g., [9], and so, can be negligible, compared to the hydrodynamic turbulence diffusion, which is quadratic in the field.] The  $\psi$  field can significantly alter the turbulent diffusion resulting from the turbulence field  $(u, v)$ . In particular, if the  $\psi$  field mainly represents a big poloidal (zonal) velocity with typical value  $v_\psi \gg v_*$ , then the particle motion will

decorrelate faster, after time  $\tau_\psi = \xi/v_\psi$ . So, the turbulent diffusion in the radial direction will have much smaller coefficient  $v_*^2\tau_\psi/2$ . At the same time, the presence of a big radial velocity component in the  $\psi$  field would significantly enhance the turbulent transport in the radial direction. The  $\psi$  field can involve many modes, including some turbulence modes; this is somewhat similar to the decomposition in [3]. Dividing modes into  $\psi$  and  $(u, v)$  components, we assume that the  $\psi$  field mainly evolves independently of the  $(u, v)$  field. [This may be due to relative magnitudes of  $\psi$  and  $(u, v)$  fields, difference in their scales, or the absence of resonance in their relative dynamics.] In the present paper, we consider the basic situation when the  $\psi$  field has just three modes. The triad interaction is basic for various phenomena and has been studied in many different contexts, in particular, in plasma [10], for water surface dynamics [11], for optical rogue waves [12], for internal waves [13], and for viscoelastic waves [14]. Thus, we assume that the  $\psi$  field consists of three modes (with complex amplitudes  $\psi_1, \psi_2, \psi_3$ ), obeying the equations

$$\begin{aligned} \dot{\psi}_1 + i\omega_1\psi_1 &= U_1\bar{\psi}_2\bar{\psi}_3 + \gamma_1\psi_1, \\ \dot{\psi}_2 + i\omega_2\psi_2 &= U_2\bar{\psi}_3\bar{\psi}_1 + \gamma_2\psi_2, \\ \dot{\psi}_3 + i\omega_3\psi_3 &= U_3\bar{\psi}_1\bar{\psi}_2; \end{aligned} \quad (2)$$

$\omega_1, \omega_2, \omega_3$  are their frequencies, and  $U_1, U_2, U_3$  are coupling coefficients, which are real numbers (the overbar denotes complex conjugation). The coefficients  $\gamma_1, \gamma_2$  are the increments (decrements) of the first two modes; the third mode represents poloidal (zonal) flow, and its increment is zero.

The purpose of the present paper is to describe a robust regime when  $F_1(t) = |\psi_1|^2$  and  $F_2(t) = |\psi_2|^2$  approach zero, while  $F_3(t) = |\psi_3|^2$  grows to large value  $F_3^*$ . In this regime, the system (2) approaches stable equilibrium, which cannot be found by solving the corresponding algebraic system, with  $\dot{F}_1 = \dot{F}_2 = \dot{F}_3 = 0$ . Indeed, system (2) is satisfied when  $\psi_1 = \psi_2 = 0$  and  $\psi_3 = c_3^* \exp(-i\omega_3 t)$  with an arbitrary constant  $c_3^*$  and correspondingly arbitrary  $F_3^* = |c_3^*|^2$ . Throughout the paper, superscript “ $\star$ ” marks the final (equilibrium) values, while superscript “0” marks the initial values.  $F_3^*$  appears to continuously depend on the initial conditions, indicating the

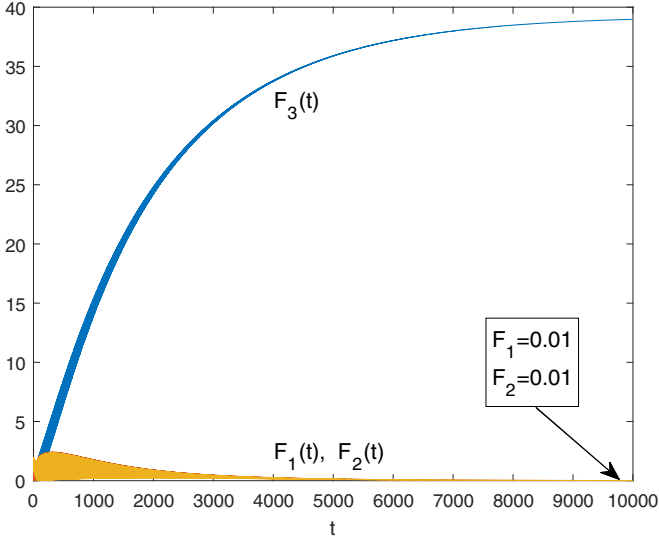


FIG. 1. The typical evolution. For this particular graph, we used  $\omega_1 = 1$ ,  $\omega_2 = -0.5$ ,  $\omega_3 = 0$ ,  $U_2 = U_3 = -U_1 = 1$ ,  $\gamma_1 = 0.006$ ,  $\gamma_2 = -0.007$  and the initial values  $F_1^0 = 1.1$ ,  $F_2^0 = 0.9$ ,  $F_3^0 = 0$ . The graph of  $F_1(t)$  is almost invisible behind the graph of  $F_2(t)$ .

presence of a conservation law in the dissipative system (2) [cf. conservation in the system (7) below].

Figure 1 shows the typical behavior. The graph shows the curves having some widths, that decrease with time. This is because the quantities  $F_1$ ,  $F_2$ ,  $F_3$  oscillate in time, and the period of oscillations is much smaller than the simulation time. As we will see later, these oscillations are ubiquitous. Their frequency increases, while their magnitude decreases.

We assume that  $U_2$  and  $U_3$  have the same sign, opposite to the sign of  $U_1$ . Then (e.g., [15,16]) the dynamics of system (2) involves two processes: (i) decay of one quantum of the first mode into one quantum of the second mode and one quantum of the third mode, as well as (ii) the inverse process. We expect that  $\gamma_1 > 0$  and  $\gamma_2 < 0$ .

Then an external source will generate energy of the first mode; this energy will transfer into both modes No. 2 and No. 3; the energy in mode No. 2 will be dissipated, while the energy supply to mode No. 3 will make this mode grow to a large magnitude. The decrement of the second mode makes both modes No. 1 and No. 2 to vanish eventually, leaving only mode No. 3 of large magnitude. For this to happen, we require that

$$\gamma \equiv \gamma_1 + \gamma_2 < 0.$$

The third mode (with zero increment) is found to grow to a larger equilibrium magnitude  $F_3^*$  if  $|\gamma|$  is much smaller than  $\gamma_1$  and  $|\gamma_2|$ , i.e., decrement almost balances increment:  $\gamma_2 \approx -\gamma_1$  (see Fig. 1).

## II. OSCILLATIONS IN SLOWLY CHANGING POTENTIAL

Let us write the system (2) in terms of the variables  $F_j$  ( $j = 1, 2, 3$ ),  $G = \text{Im}(\psi_1\psi_2\psi_3)$ , and

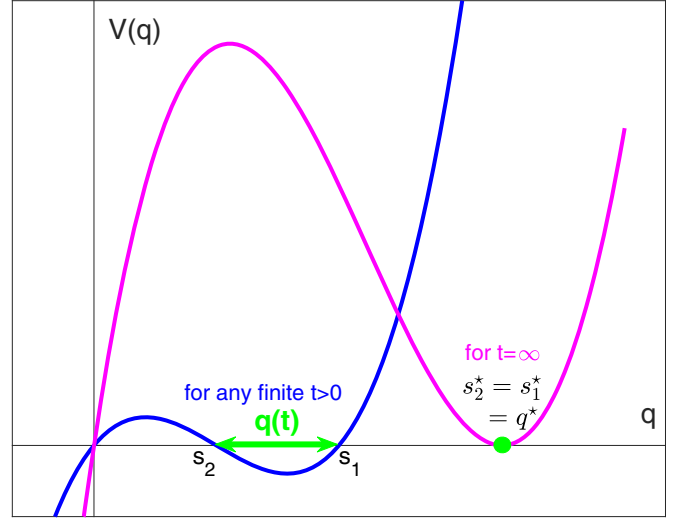


FIG. 2. Sketch of the dynamics in system (6).

$H = \text{Re}(\psi_1\psi_2\psi_3)$ :

$$\begin{aligned} \dot{F}_1 &= 2U_1H + 2\gamma_1F_1, & \dot{F}_2 &= 2U_2H + 2\gamma_2F_2, \\ \dot{F}_3 &= 2U_3H, & \dot{G} &= -\omega H + \gamma G, \\ \dot{H} &= \omega G + \gamma H + U_1F_2F_3 + U_2F_3F_1 + U_3F_1F_2, \end{aligned} \quad (3)$$

where  $\omega \equiv \omega_1 + \omega_2 + \omega_3$ . The system (3) is subject to the obvious constraint

$$R \equiv G^2 + H^2 - F_1F_2F_3 = 0. \quad (4)$$

It is consistent with the dynamics (3):  $\dot{R} = 2\gamma R$ , so that if  $R = 0$  initially, it will remain zero.

We need to distinguish between resonant ( $\omega = 0$ ) and nonresonant cases.

### A. Resonant case

When  $\omega = 0$ , the fourth equation in system (3) implies that  $G$  approaches zero. Let us assume that  $G^0 = 0$ , and then  $G \equiv 0$ .

Now consider variables

$$s_1 = a \left( \frac{F_3}{U_3} - \frac{F_1}{U_1} \right), \quad s_2 = a \left( \frac{F_3}{U_3} - \frac{F_2}{U_2} \right), \quad q = a \frac{F_3}{U_3} \quad (5)$$

with some constant  $a$  that we choose later. Then the system (3),(4) can be written in the form

$$\dot{s}_1 = 2\gamma_1(s_1 - q), \quad \dot{s}_2 = 2\gamma_2(s_2 - q), \quad (\dot{q})^2 + V(q) = 0, \quad (6)$$

where we have introduced  $V(q) = q(s_1 - q)(s_2 - q)$  and chosen  $a = -4U_1U_2U_3$ . In system (6), the equation with  $\dot{q}$  represents the constraint (4). The time differentiation of this equation gives the last equation of the system (3), for  $\dot{H}$ . This is because  $H = \dot{q}/2a$  according to the third equation in (3). The system (6) has a simple physical meaning (Fig. 2): The particle with coordinate  $q$  and mass 2 oscillates in cubic potential  $V(q)$ , while the roots of the cubic are slowly moving. Eventually,  $s_2$  and  $s_1$  coalesce, fixing the oscillating particle:

$s_2^* = s_1^* = q^*$ . To be specific, we assume  $U_1 < 0$ ,  $U_2 > 0$ ,  $U_3 > 0$ , and so,  $s_1 > s_2$ .

Averaging gives us

$$\dot{s}_1 = 2\gamma_1(s_1 - Q), \quad \dot{s}_2 = 2\gamma_2(s_2 - Q), \quad (7)$$

where  $Q$  is the average of  $q(t)$  over the period  $T$  of the oscillations

$$T = 2 \int_{\text{mid}}^{\text{big}} \frac{dq}{\sqrt{-V(q)}}, \quad Q = \frac{2}{T} \int_{\text{mid}}^{\text{big}} \frac{q dq}{\sqrt{-V(q)}}.$$

In both integrals, the integration is from the middle root to the biggest root of the cubic  $V(q)$ . The factor 2 in front of the integrals accounts for motion back and forth between the roots. The biggest root is  $s_1$ , and for most of the time, the middle root is  $s_2$ . But initially,  $s_2$  might be negative, and then the middle root is 0; this indeed happens if  $F_3^0 = 0$ .

The averaging should produce an accurate approximation if increment and decrement are small compared to  $T^{-1}$ . However, the period  $T$  becomes large when  $s_2$  passes through zero ( $T = \infty$  when  $s_2 = 0$ ). Computer simulations show that this event (if it actually occurs) can be disregarded, and averaging works on the whole interval  $0 < t < \infty$ .

The system (7) is invariant under multiplication of variables  $s_1, s_2$  by the same constant  $b$ . [To see this, one can change the integration variable  $q \rightarrow bq$  in the integrals for  $T, Q$  and observe that  $Q(bs_1, bs_2) = bQ(s_1, s_2)$ .] This continuous symmetry leads to a conservation law.

As  $t \rightarrow \infty$ , the system (7) equilibrates to the state  $s_1^* = s_2^* = h$ , where  $h = q^* = Q(s_1^*, s_2^*)$  is undetermined (it depends on the initial conditions). Near the equilibrium, the graph of  $V(q)$  within the interval  $s_2 < q < s_1$  is approximately parabola, and the average  $Q$  approximately equals  $(s_1 + s_2)/2$ . Then system (7) becomes

$$\dot{s}_1 = \gamma_1(s_1 - s_2), \quad \dot{s}_2 = \gamma_2(s_2 - s_1).$$

**B. Nonresonant case**

When  $\omega \neq 0$ , we introduce one more variable  $s_3 = a(F_3/U_3 + 2G/\omega)$  in addition to  $s_1, s_2, q$  defined in (5). Choosing  $a = -4U_1U_2U_3/\omega^2$ , we rewrite the system (3),(4) as

$$\begin{aligned} \dot{s}_1 &= 2\gamma_1(s_1 - q), & \dot{s}_2 &= 2\gamma_2(s_2 - q), \\ \dot{s}_3 &= \gamma(s_3 - q), & (\dot{q}/\omega)^2 + V(q) &= 0 \end{aligned} \quad (8)$$

with function

$$V(q) = (s_3 - q)^2 + q(s_1 - q)(s_2 - q). \quad (9)$$

Again, system (8) has a simple physical interpretation (Fig. 3): The particle with coordinate  $q$  and mass  $2/\omega^2$  oscillates in the cubic potential  $V(q)$ , while the coefficients of the potential are slowly changing. The roots of the cubic, enumerated in decreasing order  $\alpha_1 \geq \alpha_2 \geq \alpha_3$ , satisfy inequality  $\alpha_3 \leq s_2 \leq \alpha_2 \leq \alpha_1 \leq s_1$ . [This is because the quadratic part of the potential (9) is positive, and the entire potential is negative in more narrow intervals than its cubic part.] The particle oscillates in the potential well, between  $\alpha_2$  and  $\alpha_1$ , with zero total (= kinetic + potential) energy. The roots are slowly moving, and eventually  $\alpha_2$  and  $\alpha_1$  coalesce, fixing the oscillating

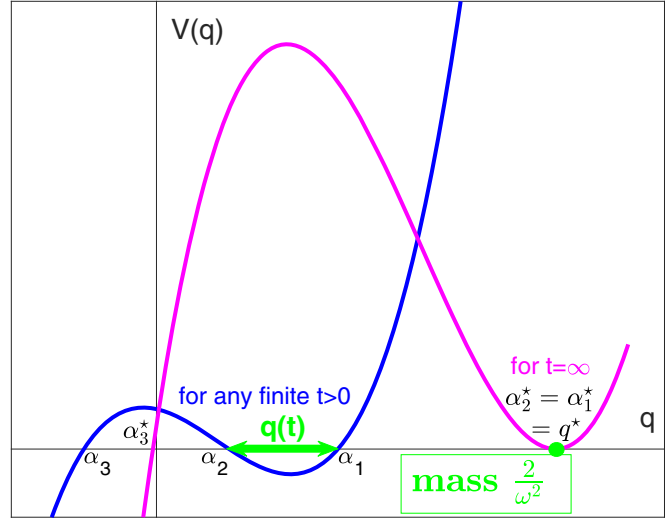


FIG. 3. Sketch of the dynamics in system (8).

particle:  $\alpha_2^* = \alpha_1^* = q^*$ . Averaging gives us

$$\dot{s}_1 = 2\gamma_1(s_1 - Q), \quad \dot{s}_2 = 2\gamma_2(s_2 - Q), \quad \dot{s}_3 = \gamma(s_3 - Q) \quad (10)$$

with  $Q$  being the average of  $q(t)$  over the oscillations

$$T = \frac{2}{|\omega|} \int_{\alpha_2}^{\alpha_1} \frac{dq}{\sqrt{-V(q)}}, \quad Q = \frac{2}{|\omega|T} \int_{\alpha_2}^{\alpha_1} \frac{q dq}{\sqrt{-V(q)}}.$$

The average  $Q$  is independent of  $\omega$  (as well as of other parameters  $\omega_1, \omega_2, \omega_3, U_1, U_2, U_3, \gamma_1, \gamma_2$ ); it depends only on the variables  $(s_1, s_2, s_3)$ .

If  $F_3^0 = 0$ , then the cubic (9) has three real roots initially. Indeed,  $F_3^0 = 0 \Rightarrow \psi_3^0 = 0 \Rightarrow G^0 = 0 \Rightarrow s_3^0 = 0$ ; also  $s_1^0 = -aF_1^0/U_1 > 0$  and  $s_2^0 = -aF_2^0/U_2 < 0$ . So,  $V^0(q) = q[q + (s_1^0 - q)(s_2^0 - q)]$  and  $\alpha_1^0 > 0, \alpha_2^0 = 0, \alpha_3^0 < 0$ .

For any  $t$ , since  $V(0) = (s_3)^2 \geq 0$  according to (9), then  $\alpha_3 \leq 0 \leq \alpha_2$ . [The other option would be  $\alpha_1 \leq 0$ . But then, according to the last equation in system (8),  $\alpha_1 \equiv q \equiv 0 \Rightarrow F_3 \equiv 0$ , and we discard this possibility.] The continuous symmetry (leading to a conservation law) of system (10)—unlike the system (7)—is unknown. This is because now the potential  $V(q)$  has both cubic and quadratic parts, and so, there appears no simple scaling for  $T$  and  $Q$ .

Equilibrium in system (10) is  $s_1^* = s_2^* = s_3^* = h$  with unknown  $h = q^*$ . The stability of the equilibrium can be investigated in the standard way by linearizing system (10). Here one needs to note that near the equilibrium, the function  $V(q)$  in the interval  $\alpha_1 < q < \alpha_2$  is essentially quadratic, and so,  $Q = (\alpha_1 + \alpha_2)/2$ . The equilibrium turns out to be stable if  $h$  is large enough, namely,  $\gamma_1 - \gamma_2 < |\gamma|\sqrt{1+h}$ .

This stability is associated with high-frequency oscillations. Indeed, near the equilibrium with large  $h$ , the potential  $V(q)$  in the interval  $\alpha_2 < q < \alpha_1$  contains a large (almost constant) factor  $(q - \alpha_3)$ . This is because  $\alpha_3$  remains negative, while  $\alpha_1, \alpha_2$  approach big positive  $h$ . So, the integral for period  $T$  gives small value.

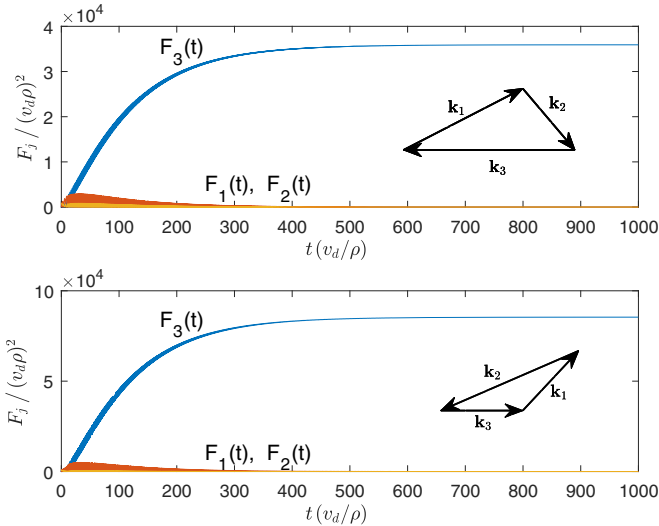


FIG. 4. The emergence of poloidal (zonal) flow due to interaction of three drift waves: (a)  $k_2 < k_1 < k_3$  and (b)  $k_3 < k_1 < k_2$  correspond to the triads (11) and (12), respectively; the triads are schematically shown inside the figures.

### III. ESTIMATE AND DISCUSSION

Now we return to the problem of plasma confinement and estimate the time needed to reach large  $F_3$ . To have an order-of-magnitude estimate, we assume that the three modes are drift waves [1] with drift velocity  $v_d = 2$  km/s, ion inertial (Rossby) radius  $\rho = 3$  mm (these are ITER values), and dimensionless wave vectors

$$\rho \mathbf{k}_1 = (2\kappa, 2\kappa), \quad \rho \mathbf{k}_2 = (\kappa, -2\kappa), \quad \rho \mathbf{k}_3 = (-3\kappa, 0) \quad (11)$$

( $\mathbf{k}_1 + \mathbf{k}_2 + \mathbf{k}_3 = 0$ ), where  $\kappa$  is a dimensionless wave number parameter; we take  $\kappa = 1/4$ . We assume  $F_2^0 \sim F_1^0 \sim 1000(v_d \rho)^2$  (the estimate is largely insensitive to the particular values of these initial data). The third amplitude is assumed to be zero initially:  $F_3^0 = 0$ . We also assume  $\gamma_1 = 0.1(v_d/\rho)$  and  $\gamma_2 = -0.11(v_d/\rho)$ . Figure 4(a) shows the emergence

of the poloidal (zonal) mode in this situation. Figure 4(b) presents a different arrangement, when

$$\rho \mathbf{k}_1 = (3\kappa, 2\kappa), \quad \rho \mathbf{k}_2 = (-6\kappa, -2\kappa), \quad \rho \mathbf{k}_3 = (3\kappa, 0) \quad (12)$$

(all parameters and initial data being the same). These graphs show that within  $10^{-4}$  s, the quantity  $F_3$  becomes an order of magnitude bigger than  $F_1, F_2$ . The above values for increment (decrement) are similar to the values assumed in the simulations [17] and to the values observed experimentally [18]. Besides, a variety of different values of  $\gamma_1, \gamma_2$  leads to the domination of  $F_3$  if  $|\gamma_1 + \gamma_2|$  is sufficiently small, compared to  $\gamma_1$  and  $|\gamma_2|$ .

It is interesting to see the generation of a dominating poloidal (zonal) component when the  $\psi$  field in Eqs. (1) has more than three modes. Such generation indeed takes place in the system of many weakly interacting drift waves [19,20]. The argument [21–23] for the emergence of poloidal (zonal) flow assumes the presence of disparate scales. Reference [24] suggests that this emergence could take place even without a difference in scales—when the range of  $\psi$  modes is limited. For this to happen, the increment (decrement) should supply a significant amount of the energy, while supplying a negligible amount of the extra invariant. Such supply requires significant decrement along with increment of other modes. The supply is feasible since the extra invariant is essentially anisotropic, unlike the energy. In this situation, the system would accumulate the energy in the poloidal (zonal) flow; this is the only place (in the wave-number plane) where the system can have the energy without the extra invariant.

In the present paper, instead of many small-amplitude waves, we considered the opposite limiting situation, when the  $\psi$  field has only three modes, but of large magnitudes.

It is also worth noting that the graphs  $F_1(t), F_2(t), F_3(t)$  look quite similar in various simulations and regular after averaging; so, further analytic progress might be possible.

### ACKNOWLEDGMENT

I benefited from discussions with A. Treibergs and G. Gustafson.

- [1] W. Horton, *Turbulent Transport in Magnetized Plasmas* (World Scientific, Singapore, 2012).
- [2] R. Marino, A. Pouquet, and D. Rosenberg, *Phys. Rev. Lett.* **114**, 114504 (2015).
- [3] J. B. Marston, G. P. Chini, and S. M. Tobias, *Phys. Rev. Lett.* **116**, 214501 (2016).
- [4] L.-A. Coustou, D. Lecoanet, B. Favier, and M. Le Bars, *Phys. Rev. Lett.* **120**, 244505 (2018).
- [5] Z. Yan, G. R. McKee, R. Fonck, P. Gohil, R. J. Groebner, and T. H. Osborne, *Phys. Rev. Lett.* **112**, 125002 (2014).
- [6] J. C. Hillesheim, E. Delabie, H. Meyer, C. F. Maggi, L. Meneses, E. Poli, and JET Contributors (EUROfusion Consortium, JET, Culham Science Centre, Abingdon, Oxon OX14 3DB, United Kingdom), *Phys. Rev. Lett.* **116**, 065002 (2016).
- [7] B. Schmid, P. Manz, M. Ramisch, and U. Stroth, *Phys. Rev. Lett.* **118**, 055001 (2017).
- [8] M. B. Isichenko, *Rev. Mod. Phys.* **64**, 961 (1992).
- [9] A. M. Balk, *J. Fluid Mech.* **467**, 163 (2002).
- [10] V. Sokolov and A. K. Sen, *Phys. Rev. Lett.* **113**, 095001 (2014).
- [11] F. Haudin, A. Cazaubiel, L. Deike, T. Jamin, E. Falcon, and M. Berhanu, *Phys. Rev. E* **93**, 043110 (2016).
- [12] S. Chen, F. Baronio, J. M. Soto-Crespo, P. Grelu, M. Conforti, and S. Wabnitz, *Phys. Rev. A* **92**, 033847 (2015).
- [13] T. Dauxois, S. Joubaud, P. Odier, and A. Venaille, *Ann. Rev. Fluid Mech.* **50**, 131 (2018).
- [14] L. Deike, M. Berhanu, and E. Falcon, *Phys. Rev. Fluids* **2**, 064803 (2017).

- [15] M. S. Longuet-Higgins and A. E. Gill, *Proc. R. Soc. London, Ser. A* **299**, 120 (1967).
- [16] A. A. Galeev and R. Z. Sagdeev, *Nonlinear Plasma Theory* (Benjamin, New York, 1969).
- [17] W. Horton and Y. H. Ichikawa, *Chaos and Structures in Nonlinear Plasmas* (World Scientific, Singapore, 1996).
- [18] W. Horton and S. Benkadda, *ITER Physics* (World Scientific, Singapore, 2015).
- [19] A. M. Balk, S. V. Nazarenko, and V. E. Zakharov, *Phys. Lett. A* **152**, 276 (1991).
- [20] A. M. Balk, *Phys. Lett. A* **155**, 20 (1991).
- [21] A. M. Balk, *Phys. Lett. A* **345**, 154 (2005).
- [22] S. Nazarenko and B. Quinn, *Phys. Rev. Lett.* **103**, 118501 (2009).
- [23] I. Saito and K. Ishioka, *Phys. Fluids* **25**, 076602 (2013).
- [24] A. M. Balk, *Astrophys. J.* **796**, 143 (2014).